AGU100 ADVANCING EARTH AND SPACE SCIENCE

JGR

Journal of Geophysical Research: Atmospheres

RESEARCH ARTICLE
10.1029/2017JD027735

Key Points:
- Obvious increasing trends in the magnitude of precipitation extreme indices are projected for most regions of Canada
- Projected changes in total precipitation are primarily caused by future changes in wind velocity and relative humidity
- Changes in precipitation extreme indices are commonly attributed to the changes in the saturation vapor pressure due to warmer temperature

Correspondence to:
G. Huang,
huangg@uregina.ca

Citation:
Zhou, X., Huang, G., Wang, X., & Cheng, G. (2018). Future changes in precipitation extremes over Canada: Driving factors and inherent mechanism. *Journal of Geophysical Research: Atmospheres*, *123*, 5783–5803. https://doi.org/10.1029/2017JD027735

Received 14 SEP 2017
Accepted 5 MAY 2018
Accepted article online 15 MAY 2018
Published online 4 JUN 2018

Future Changes in Precipitation Extremes Over Canada: Driving Factors and Inherent Mechanism

Xiong Zhou[1], Guohe Huang[1], Xiuquan Wang[2], and Guanhui Cheng[1]

[1]Institute for Energy, Environment and Sustainable Communities, University of Regina, Regina, Saskatchewan, Canada, [2]School of Climate Change and Adaptation, University of Prince Edward Island, Charlottetown, Prince Edward Island, Canada

Abstract In this study, future changes in precipitation extremes over 10 climatic regions in Canada and their mechanism under Representative Concentration Pathways (RCPs) throughout the 21st century are investigated by using the Providing Regional Climates for Impacts Studies (PRECIS) model. The performance of PRECIS in hindcasting total and extreme precipitation for the historical period is first evaluated through two experiments driven by the boundary conditions from both ERA-Interim (1979–2011) and HadGEM2-ES (1959–2005). The validation results indicate that PRECIS can reasonably reproduce both the magnitudes and spatial patterns of precipitation extremes over Canada. Changes in total and extreme precipitation for two future periods are analyzed to explore how regional climate over different climatic regions would respond to global warming. Mechanism governing changes in precipitation extremes is explored through a comprehensive analysis of potential climate factors and their correlations and interactions with precipitation extremes. There are obvious increasing trends over most regions for the magnitude of precipitation extremes except for the duration indices. Averages of projected precipitation extremes over the climatic regions in Canada are projected to increase under RCP4.5. Such increases under RCP8.5 would be amplified due to higher greenhouse gas emissions. The projected changes in total precipitation are dominated by changes in wind velocity and relative humidity (e.g., changes in horizontal water vapor flux that would have significant effects on the occurrence of precipitation in Canada). In addition, the changes in the majority of precipitation extremes are commonly attributed to the changes in the saturation vapor pressure due to warmer temperature as described by the Clausius-Clapeyron equation.

1. Introduction

Impacts of climate change on precipitation extremes have been of concern to many researchers in recent decades (Bao et al., 2015; Hartmann et al., 2013; Held & Soden, 2006; Qin & Xie, 2016; Seager et al., 2007). Canada is now suffering tremendous amounts of damage due to more frequent and severe precipitation extremes (Held & Soden, 2006; Seager et al., 2007; Wang et al., 2015; Zhou, Huang, Wang, et al., 2018). Recently, regional climate models (RCMs) have been widely employed to analyze the potential impacts of climate change under the Representative Concentration Pathways (RCPs; Van Vuuren et al., 2011). RCMs are able to simulate regional atmospheric and terrestrial processes (Denis et al., 2002; Jones et al., 1995). Therefore, it requires a better understanding of how climate change will affect extreme precipitation in Canada (Intergovernmental Panel on Climate Change, 2013; Maurer et al., 2007).

Over the past decade, RCMs have been widely used to study local climate and extreme events over Canada (Jeong, Sushama, Diro, & Khaliq, 2016; Jeong, Sushama, Diro, Khaliq, Beltrami, et al., 2016; Mladjic et al., 2011; Plummer et al., 2006; Sushama et al., 2010; Zhou, Huang, Wang, et al., 2018). For example, Zhou, Huang, Wang, et al. (2018) dynamically downscaled temperature and precipitation changes over Saskatchewan, Canada, based on the PRECIS model. Jeong, Sushama, Diro, and Khaliq (2016) investigated the impact of climate change on cold extreme days (i.e., cold nights, cold days, frost days, and ice days) and cold spells over Canada based on 11 RCMs. Jeong, Sushama, Diro, Khaliq, Beltrami, et al. (2016) analyzed the projected changes in hot days, hot spells, and heat waves in a Canadian context by using 11 RCM simulations from the North American Regional Climate Change Assessment Program. Wang et al. (2015) developed high-resolution climate projections over Ontario, Canada, to assess plausible impacts of climate change through an ensemble modeling approach. Mladjic et al. (2011) developed projections of extreme precipitation changes over Canada for the Special Report on Emissions Scenarios A2 by using the Canadian Regional Climate Model.

Most of previous studies on the Canadian precipitation climate as simulated by climate models were based on Special Report on Emissions Scenarios. In addition, there have been few studies to investigate future changes and inherent mechanism in precipitation extremes over the Canadian climatic regions for RCPs as recommended by Intergovernmental Panel on Climate Change (2013). According to Environment and Climate Change Canada (2016), warming rates in Canada are about twice the global rate for centuries due to long-lived greenhouse gases (GHGs) and warming oceans. Moreover, changes in precipitation extremes, floods, and droughts will have significant impacts on society, leading to environmental hazards and severe disruptions in economic activities (Fan et al., 2017; Mladjic et al., 2011; Shabbar & Bonsal, 2003). It is thus necessary to explore the impact of warmer climate on precipitation extremes over Canada and the inherent mechanism for RCPs.

Therefore, the objective of this study is to analyze the changes in precipitation extremes over climatic regions in Canada as well as their driving factors and inherent mechanism for both RCPs throughout this century through a dynamical downscaling approach. In detail, the PRECIS model will be adopted to dynamically downscale of ERA-Interim (1979–2011) and HadGEM2-ES (1959–2005) over the entirety of Canada. The performance of PRECIS in hindcasting annual mean and extreme precipitation for the historical period of 1986–2005 will then be evaluated through comparisons with observations. PRECIS will be employed to conduct simulations for the period of 2005–2099, driven by the boundary conditions from HadGEM2-ES for both RCP4.5 and RCP8.5. Changes in annual mean and extreme precipitation for two future periods (i.e., 2036–2065 and 2066–2095) will also be analyzed to help explore how regional climate over 10 climatic regions would respond to global warming. Moreover, mechanism governing the projected changes in precipitation extremes is revealed through a comprehensive analysis of the potential climate factors and their correlations and interactions with precipitation extremes. The projected changes and revealed mechanism in precipitation extremes over Canada can be helpful in understanding the major atmospheric phenomena across Canada and their physical processes at regional and local scales.

2. Methodology

The PRECIS model developed by the UK Hadley Centre is employed to generate high-resolution physically based climate projections over Canada. There are two different horizontal resolutions in the PRECIS model: $0.44° \times 0.44°$ and $0.22° \times 0.22°$, which can provide a minimum resolution of 50 km × 50 km and 25 km × 25 km, respectively (Centella-Artola et al., 2015; Wang, Huang, Lin, et al., 2014). The PRECIS model includes 19 levels described by a combination of σ coordinate and pressure coordinate (Wilson et al., 2005). The framework builds upon a primitive hydrostatic equation grid point model. The land surface model is the Met Office Surface Exchange Scheme (Cox et al., 1999). The mass flux penetrative scheme with an explicit downdraught is employed as the convective scheme (Jones et al., 1995). The radiation scheme is composed of the seasonal and diurnal cycles of insolation for computing short wave and long wave fluxes (Jones & Hassell, 2004). The detailed model parameterization is described by Jones and Hassell (2004). The PRECIS model has been widely employed to generate detailed regional climate change projections for impact studies (Jones & Hassell, 2004; Zhou, Huang, Wang, et al., 2018).

The ERA-Interim (1979 to 2011), HadGEM2-ES historical experiment (1959–2005), and future experiments for RCPs (2006–2099) are employed as the initial and lateral boundary conditions of PRECIS. PRECIS requires large inputs of computing resources and data storage to downscale GCMs to a 25-km resolution. Moreover, previous work suggests that there are only modest improvements in reflecting local precipitation events with resolution from 50 to 25 km (Zhou, Huang, Baetz, et al., 2018; Zhou, Huang, Wang, et al., 2018; Zhou et al., 2017). The PRECIS experiment is thus performed at a horizontal resolution of $0.44° \times 0.44°$ (i.e., 50 km). There are 131 (longitude) × 113 (latitude) grid points in the experimental domain over North America covering the entirety of Canada. The data for period of 1986–2005 are extracted to represent the baseline period according to Intergovernmental Panel on Climate Change (2013). Changes in precipitation extremes from the PRECIS simulations for both RCP4.5 and RCP8.5 are analyzed for the 2050s (2036–2065) and 2080s (2066–2095).

Moreover, the Canadian climatic regions are used in this study to help further understand precipitation changes at the regional scale. These regions are defined based on climatic homogeneity (Plummer et al., 2006) and have been employed in many studies to analyze precipitation and temperature extremes (Jeong, Sushama, Diro, Khaliq, Beltrami, et al., 2016; Mailhot et al., 2012; Mladjic et al., 2011; Plummer et al., 2006). Figure 1 shows the domain and the topography in the Canadian climatic regions: Yukon (YUK), Mackenzie (MAC), Arctic (ARC), Pacific coast (PAC), South British Columbia mountains (SBC), Northwestern

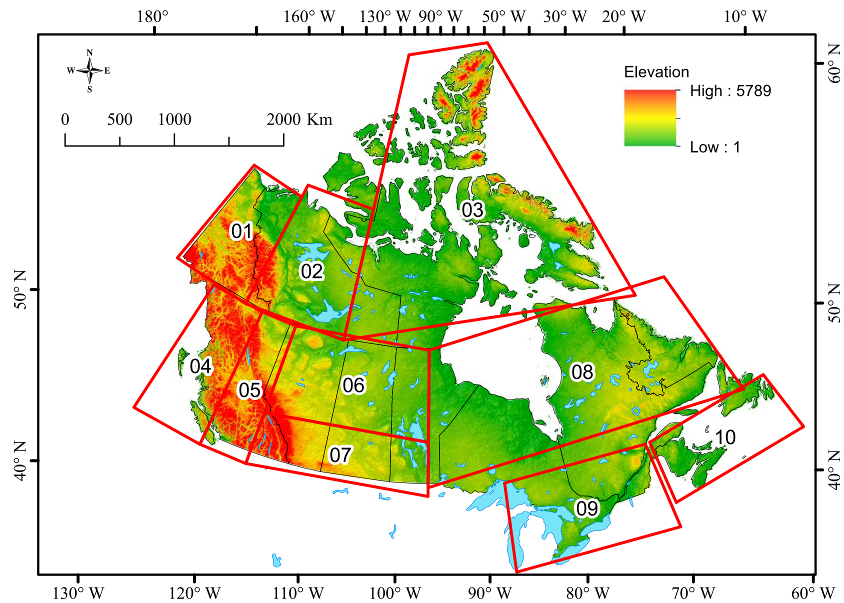

Figure 1. Topography and climatic regions in the study area: 01 Yukon (YUK), 02 Mackenzie (MAC), 03 Arctic (ARC), 04 Pacific coast (PAC), 05 South British Columbia mountains (SBC), 06 Northwestern forest (NWF), 07 Prairies (PAI), 08 Northeastern forest (NEF), 09 Great Lakes (GLK), and 10 Atlantic (ATL).

forest (NWF), Prairies (PAI), Northeastern forest (NEF), Great Lakes (GLK), and Atlantic (ATL). For example, the PAI climate is mostly dry with long cold winters and short hot summers (Zhou, Huang, Wang, et al., 2018), while the PAC climate is cool in summer and mild in winter.

In order to better analyze extreme events over Canada, 10 precipitation extreme indices are derived from the Expert Team on Climate Change Detection and Indices (Frich et al., 2002; Sillmann, Kharin, Zhang, et al., 2013). In the past, the precipitation extreme indices have been widely employed in climate research studies (Bao et al., 2015; Li et al., 2013; Qin & Xie, 2016; Sillmann, Kharin, Zhang, et al., 2013; Sillmann, Kharin, Zwiers, et al., 2013). In detail, the precipitation extreme indices in this study can be classified into the following categories: (i) absolute indices (Rx1day and Rx5day), (ii) threshold indices (R10mm and R20mm), (iii) percentile indices (R95pTOT and R99pTOT), (iv) duration indices (CDD and CWD), and (v) other two indices (SDII and PRCPTOT; Qin & Xie, 2016; Sillmann, Kharin, Zhang, et al., 2013). Table 1 provides the detailed definition of 10 precipitation extreme indices.

To evaluate the capability of PRECIS in hindcasting historic observations in the Canadian context, the gridded observations of daily wind and geopotential height at 850 hPa as well as daily accumulated precipitation are derived from the North American Regional Reanalysis dataset (NARR). It is a high-resolution (i.e., 32-km) dataset for the period of 1979 to present over the North America domain (Janjić, 1994). As an extension of the National Centers for Environmental Prediction (NCEP) Global Reanalysis, the NARR dataset employed the NCEP Eta Model and the Regional Data Assimilation System to run over the North America (Mesinger et al., 1988; Saha et al., 2014). The output data can be used as gridded estimations of historical climate (Kennedy et al., 2011). In this study, the time series of daily precipitation from 1986 to 2005 were extracted to represent the historical Canadian climatology.

3. Results

3.1. Evaluation of the PRECIS Simulation

The capability of the PRECIS model in capturing the annual and seasonal mean precipitation over the Canadian context for the baseline period of 1986–2005 is first evaluated. Figure 2 presents the spatial distribution of seasonal (Figures 2-1 to 2-12) and annual (Figures 2-13 to 2-15) total precipitation from ERA-PRECIS (i.e., PRECIS driven by ERA-Interim reanalysis), Had-PRECIS (i.e., PRECIS driven by HadGEM2-ES), and the NARR dataset for the historical period. The results of the NARR dataset shown in Figure 2-15 indicate that the central and northern Canada receives relatively lower amount of annual total precipitation than the southeastern

10.1029/2017JD027735

Table 1

Ten Precipitation Extreme Indices Recommended by the Expert Team on Climate Change Detection and Indices (Sillmann, Kharin, Zhang, 2013)

Label	Index name	Index definition
Absolute indices		
Rx1day	Max 1 day precipitation	Annual maximum 1-day precipitation
Rx5day	Max 5 day precipitation	Annual maximum consecutive 5-day precipitation
Threshold indices		
R10mm	Heavy precipitation days	Annual count of days when precipitation ≥10 mm
R20mm	Very heavy precipitation days	Annual count of days when precipitation ≥20 mm
Duration indices		
CDD	Consecutive dry days	Annual maximum number of consecutive days with precipitation <1 mm:
CWD	Consecutive wet days	Annual maximum number of consecutive days with precipitation ≥1 mm:
Percentile Indices		
R95pTOT	Very wet days	Annual total precipitation when precipitation ≥95th percentile of precipitation
R99pTOT	Extremely wet days	Annual total precipitation when precipitation ≥99th percentile of precipitation
Other two indices		
SDII	Simple daily intensity	Mean precipitation on wet days
PRCPTOT	Total wet-day precipitation	Annual total precipitation on wet days

(i.e., GLK and ALC) and southwestern (i.e., PAC) Canada, where regional climates are significantly influenced by the ocean or Great lakes. There are similar spatial distribution patterns in the seasonal total precipitation.

Compared with the NARR dataset, ERA-PRECIS and Had-PRECIS could capture the general distribution patterns of annual and seasonal total precipitation. Figure 3 further presents the differences in annual/seasonal mean geopotential height and wind at 850 hPa and annual/seasonal total precipitation between simulations and observations. The results indicate that both ERA-PRECIS and Had-PRECIS underestimate annual and seasonal total precipitation in the southwestern regions, while the precipitation is overestimated in the southeastern and northeastern regions. Moreover, there are larger wet biases in the total precipitation from ERA-PRECIS than that from Had-PRECIS.

The Taylor diagram (Taylor, 2001) is used in this study to further evaluate the performance of PRECIS in simulating spatial patterns of both annual and seasonal total precipitation over the 10 regions in the Canadian context. It is capable of comparing spatial correlation coefficient, standard deviation, and root-mean-square error within a 2-D graph (Taylor, 2001). Figure 3 summarizes the comparison of the PRECIS model and NARR observations over the 10 regions in Canada. The performance in simulating precipitation over a region can be considered better if there is a closer distance to the reference object. The size of the down and up triangle respectively represents a negative and positive difference in averaged total precipitation over the domain.

The results shown in Figure 4 indicate that ERA-PRECIS and Had-PRECIS have slightly poor performance in simulating the spatial distribution patterns of annual and seasonal total precipitation over some regions. For example, the spatial distribution patterns over GLK and ATL are not very well simulated by both ERA-PRECIS and Had-PRECIS as seen from their relatively low correlations. The results in Figure 4 also indicate that there are large wet biases for annual and seasonal total precipitation over the regions of YUK, GLK, and ATL. Moreover, ERA-PRECIS and Had-PRECIS show relative lower spatial correlation in autumn total precipitation than that in other seasonal total precipitation for the majority of the regions. Overall, the PRECIS model could generally capture the spatial variability and pattern of annual and seasonal total precipitation over most regions.

In order to assess the capability of the PRECIS model in simulating precipitation extremes, the time series of daily precipitation for the historical period of 1986–2005 are first extracted from ERA-PRECIS, Had-PRECIS, and NARR. The annual precipitation extreme indices are then calculated by using the Climate Data Operators (https://code.zmaw.de/projects/cdo). Figures 5 and 6 present the comparison of historical spatial distributions for five categories of annual precipitation extreme indices over the entirety of Canada. The result of

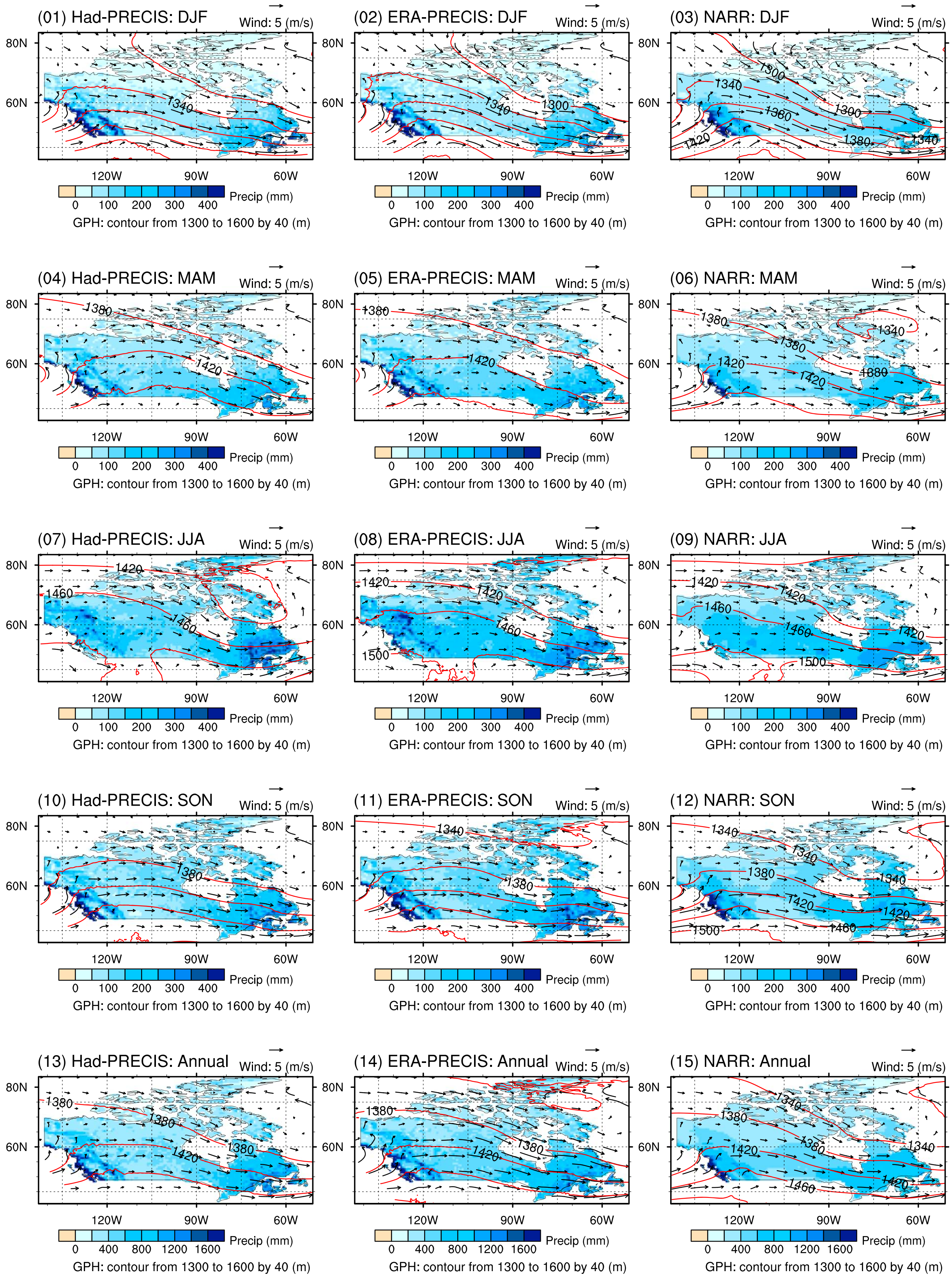

Figure 2. Spatial distributions of annual mean wind (*u* and *v*) and geopotential height at 850 hPa, as well as annual and seasonal total precipitation for 1986–2005 over Canada from ERA-PRECIS, Had-PRECIS, and observations.

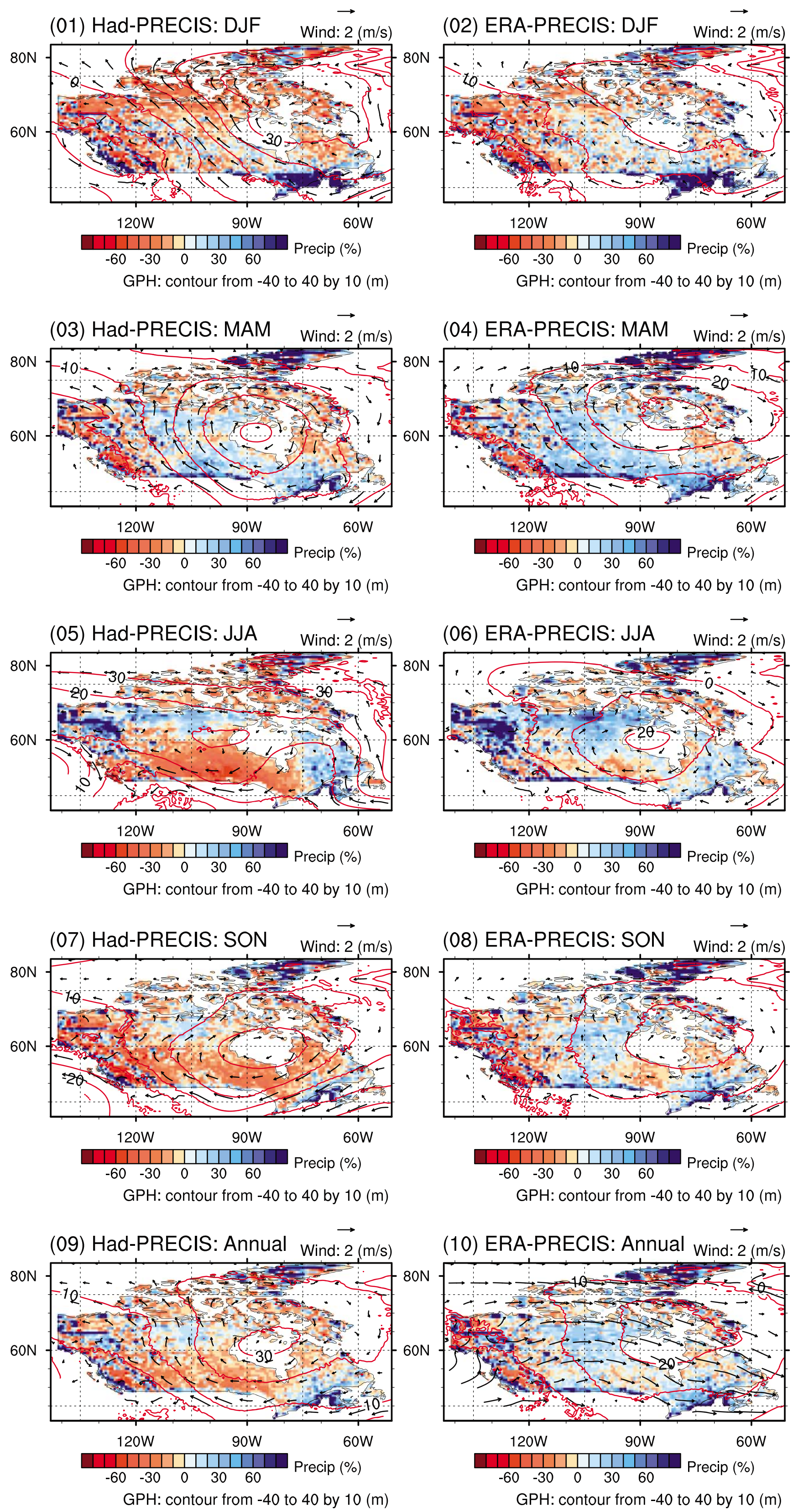

Figure 3. Difference in annual and seasonal mean geopotential height and wind at 850 hPa and annual and seasonal total precipitation between simulations and observations.

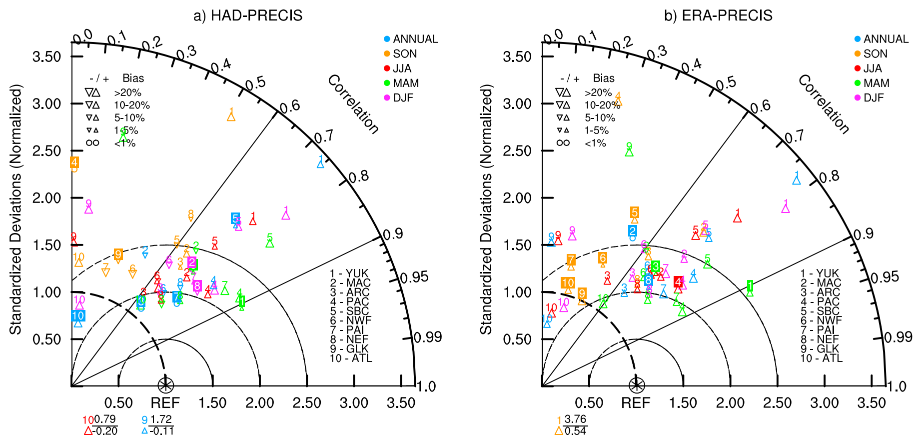

Figure 4. Taylor diagram for annual and seasonal total precipitation over 10 climatic regions from ERA-PRECIS and Had-PRECIS for the historical period.

the NARR dataset presented in Figure 5-15 shows a discontinuity at the Canada-U.S. border. This is because NARR assimilates a lower resolution of station data from Canada than those from the United States.

The results indicated that the precipitation extreme indices excluding the CDD show a similar distribution pattern with the annual and seasonal precipitation. The values of these indices over the southeastern and southwestern Canada are relatively higher than those over the central and northern Canada. This is primarily a consequence of spatial patterns in total precipitation over Canada. In general, ERA-PRECIS and Had-PRECIS are capable of capturing both spatial distribution patterns and extreme precipitation magnitudes of most extreme indices through the comparison with the NARR dataset. Apart from CWD (Figures 6-1 to 6-3), the magnitudes of the precipitation extreme indices are slightly overestimated by the PRECIS downscaling. This is especially true for the simulation over the southeastern and southwestern Canada. Nevertheless, the PRECIS simulation underestimates the magnitude of CWD and CDD in the southeastern Canada.

Figure 7 shows the regional averages in these extreme indices from 1986 to 2005 based on ERA-PRECIS, Had-PRECIS, and NARR. The comparison result reveals that the regional averages over the 10 regions are further agreed with the spatial distribution patterns of these extreme indices. It can be observed that both ERA-PRECIS and Had-PRECIS could not be able to simulate some of the indices very well over the Canadian climatic regions. For example, compared with the NARR observations, the simulated regional averages of R20mm (Figure 7-4) from ERA-PRECIS and Had-PRECIS are much larger than the observations. As for CDD shown in Figure 7-5, the regional averages over the GLK and ATL simulated by PRECIS are much smaller than the observations. These two regions are located in southeastern Canada. However, PRECIS performs very well in simulating magnitudes of regional averages in CWD over the 10 regions.

Overall, the validation results indicate that ERA-PRECIS and Had-PRECIS can reasonably reproduce the magnitudes and spatial patterns of precipitation extremes over Canada through comparison with the observations. Moreover, we found that PRECIS could not fully capture formation and precipitation of convective clouds and large-scale clouds over the southeastern region as seen from its slightly poor performance in simulating precipitation extremes.

3.2. Projected Changes in Precipitation Extremes

For the purpose of analyzing future changes in precipitation extremes, the precipitation projection over the Canadian domain for the future period of 2006–2099 is first developed by using the PRECIS model, driven by HadGEM2-ES under RCP4.5 and RCP8.5. The annual and seasonal total precipitation changes relative to the historical period 1986–2005 are first analyzed in two future 30-year periods: the 2050s (2036–2065) and 2080s (2066–2095). Figure 8 presents the projected changes in annual and seasonal precipitation over Canada for the period of the 2050s and 2080s under both RCPs. The results indicate that annual total precipitation under RCP4.5 is mostly projected to increase in the 2050s and 2080s over Canada. Nevertheless, the PRECIS simulation under RCP8.5 project that annual total precipitation in the 2050s and 2080s will be significantly increased over the entirety of Canada.

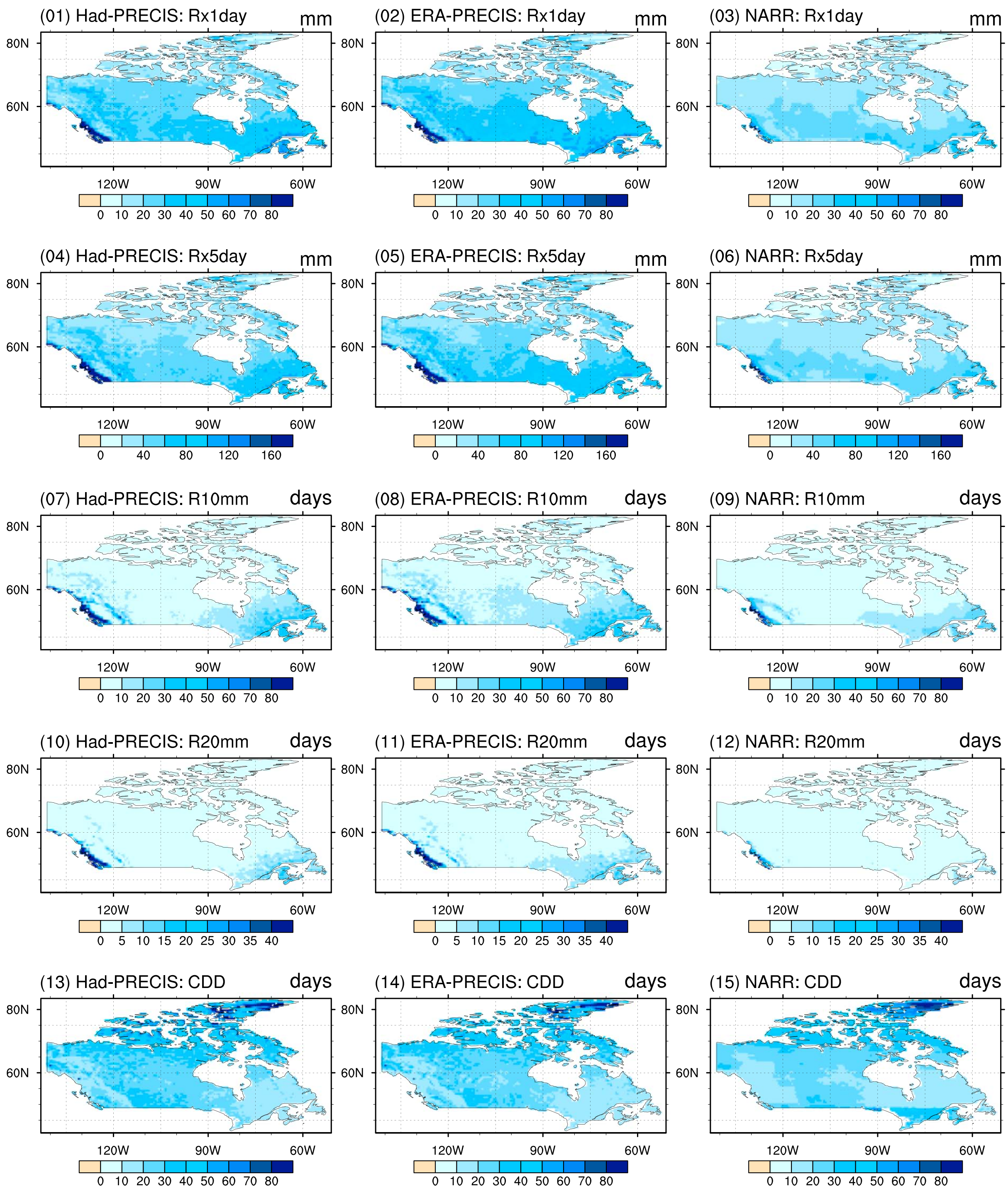

Figure 5. Spatial distribution of annual mean Rx1day, Rx5day, R10mm, R20mm, and CDD in the period of 1986–2005 over Canada from ERA-PRECIS, Had-PRECIS, and NARR.

For the projected seasonal total precipitation, larger increases are projected in winter and autumn in the 2050s and 2080s for both RCPs. Moreover, summer total precipitation for the 2050s and 2080s under RCP4.5 is projected to decrease in the southern Canada and increase in northern Canada. In contrast, PRECIS projects a larger increase in autumn total precipitation over the southern Canada in the 2050s and 2080s for both RCPs. Although there is a similar pattern in the annual and seasonal total precipitation for both RCPs, the magnitude of changes is significantly different. Specifically, due to greater GHG concentrations, the

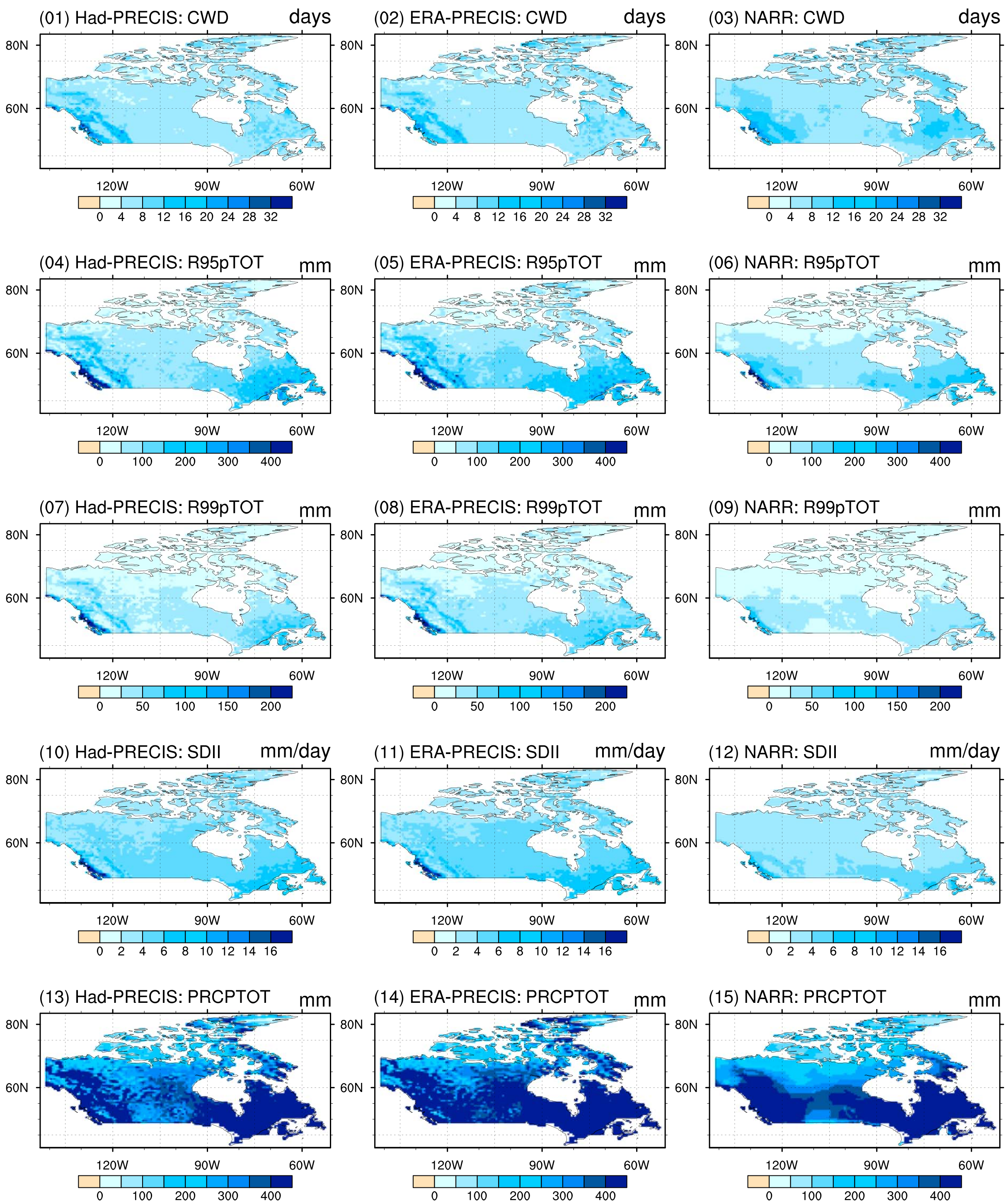

Figure 6. Spatial distribution of annual mean CWD, R95Ptot, R99Ptot, SDII, and PRCPTOT in the period of 1986–2005 over Canada from ERA-PRECIS, Had-PRECIS, and NARR.

projected changes in annual and seasonal total precipitation would be amplified under the RCP8.5 scenario. This will likely have a potential impact on the frequency of precipitation extremes.

Figure 9 presents the spatial distribution of the projected changes in 10 precipitation extreme indices over Canada for the 2050s and 2080s under RCP4.5. The results in the two future periods suggest that there is an obvious increasing trend over the majority of Canadian regions for the magnitude of precipitation

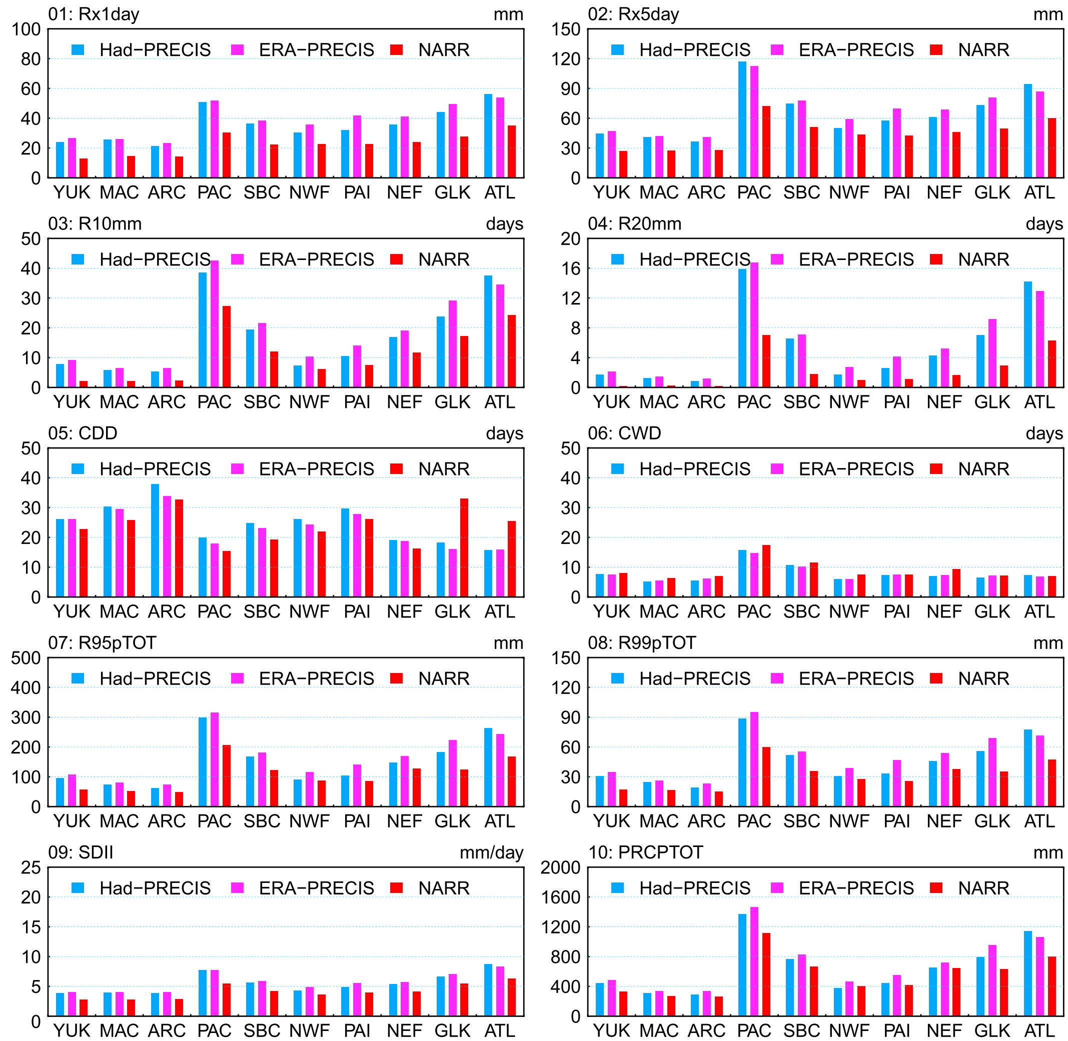

Figure 7. Regional averages of annual mean precipitation extreme indices over the climatic regions from ERA-PRECIS, Had-PRECIS, and NARR for the historical period.

extreme indices except for the duration indices (i.e., CDD and CWD). In addition to the increasing trend, the changes in magnitudes of the precipitation extreme indices show a similar pattern with the annual total precipitation under RCP4.5. This is also consistent with the results derived from the annual total precipitation. For example, the PRECIS model tends to project a decrease in the absolute indices (i.e., Rx1day and Rx5day) over the southeastern and southwestern Canada, while other regions are mostly projected an increase in the indices for the 2050s and 2080s. However, changes in magnitudes of the duration indices (i.e., CWD and CDD) show different spatial patterns. In detail, changes in CDD and CWD over many regions are projected to decrease for the 2050s and 2080s under the RCP4.5 scenario. An opposite spatial pattern is also found in the projected changes in CDD. In contrast, changes in CWD derived from the PRECIS simulation under RCP4.5 are projected to decrease more over the southeastern and southwestern Canada.

The projected changes in precipitation extreme indices under RCP8.5 are also analyzed for the future periods (i.e., 2050s and 2080s) with respect to the baseline period. Figure 10 shows the results of changes in precipitation extreme indices derived from the PRECIS simulations driven by the HadGEM2-ES global model dataset under RCP8.5. Due to the increasing sensitivity of future projections with GHG concentrations, changes in magnitudes of the precipitation extreme indices are significantly enlarged in the two future periods under RCP8.5. Moreover, the entirety of Canada for the 2050s and 2080s shows an obvious increasing trend in

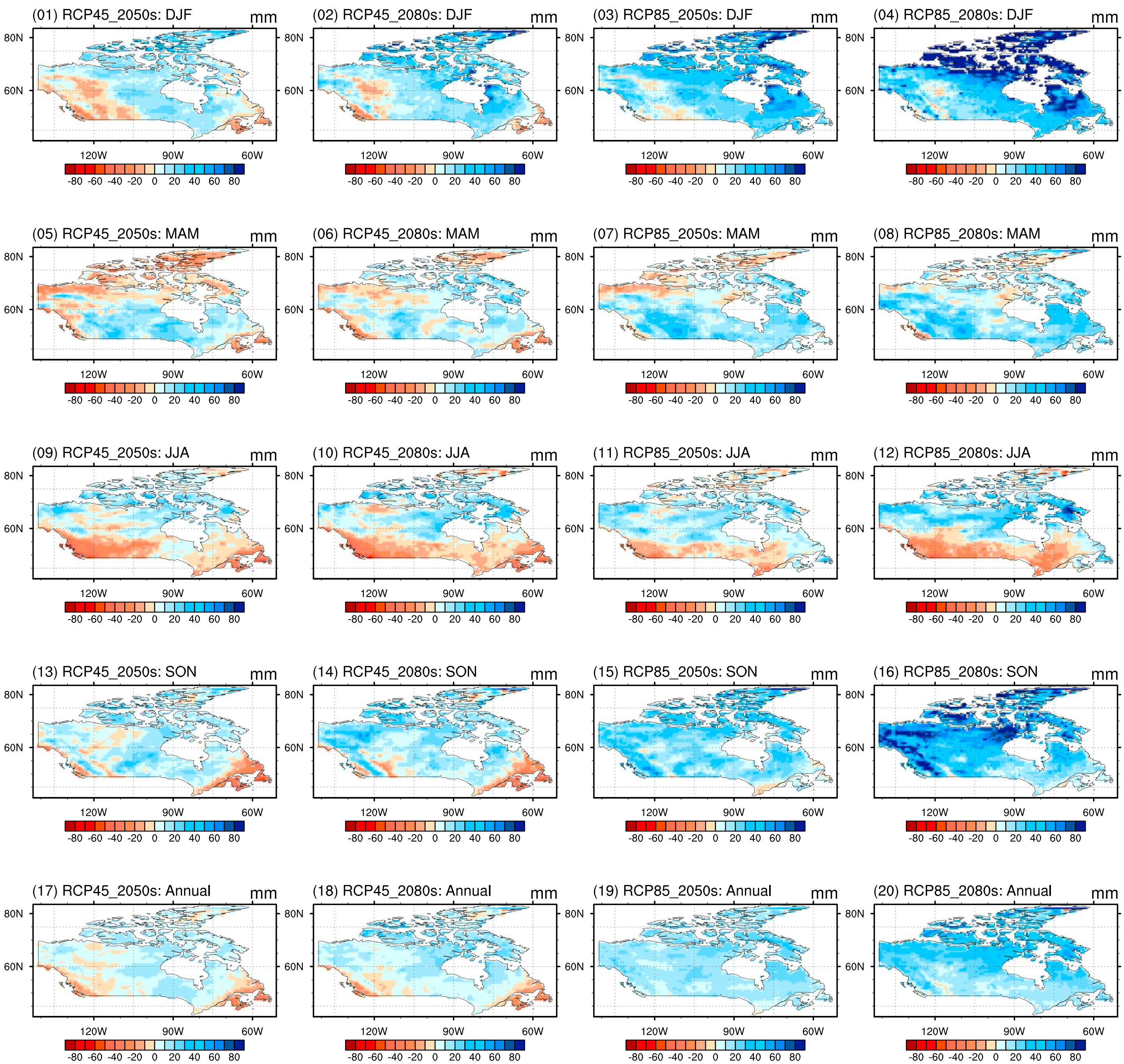

Figure 8. Spatial distribution of the projected changes in annual and seasonal total precipitation for both RCPs in the two future periods over Canada.

precipitation extreme indices excluding the duration indices. As for the changes in CDD and CWD under RCP8.5, the results indicate that there are a larger decrease in CDD and no significant changes in CWD except a decrease in the southwest in the two future periods.

Figure 11 depicts the averaged changes in precipitation extreme indices over 10 climatic regions for the two future periods for both RCPs. It is indicated that the averages of most projected precipitation extreme indices would be generally increased in the 2050s and 2080s under RCP4.5 except for PAC and ATL. The results are further agreed with the spatial distribution of the projected changes in precipitation extreme indices for both RCPs. For example, the averages of the absolute indices (i.e., Rx1day and Rx5day) in future periods are

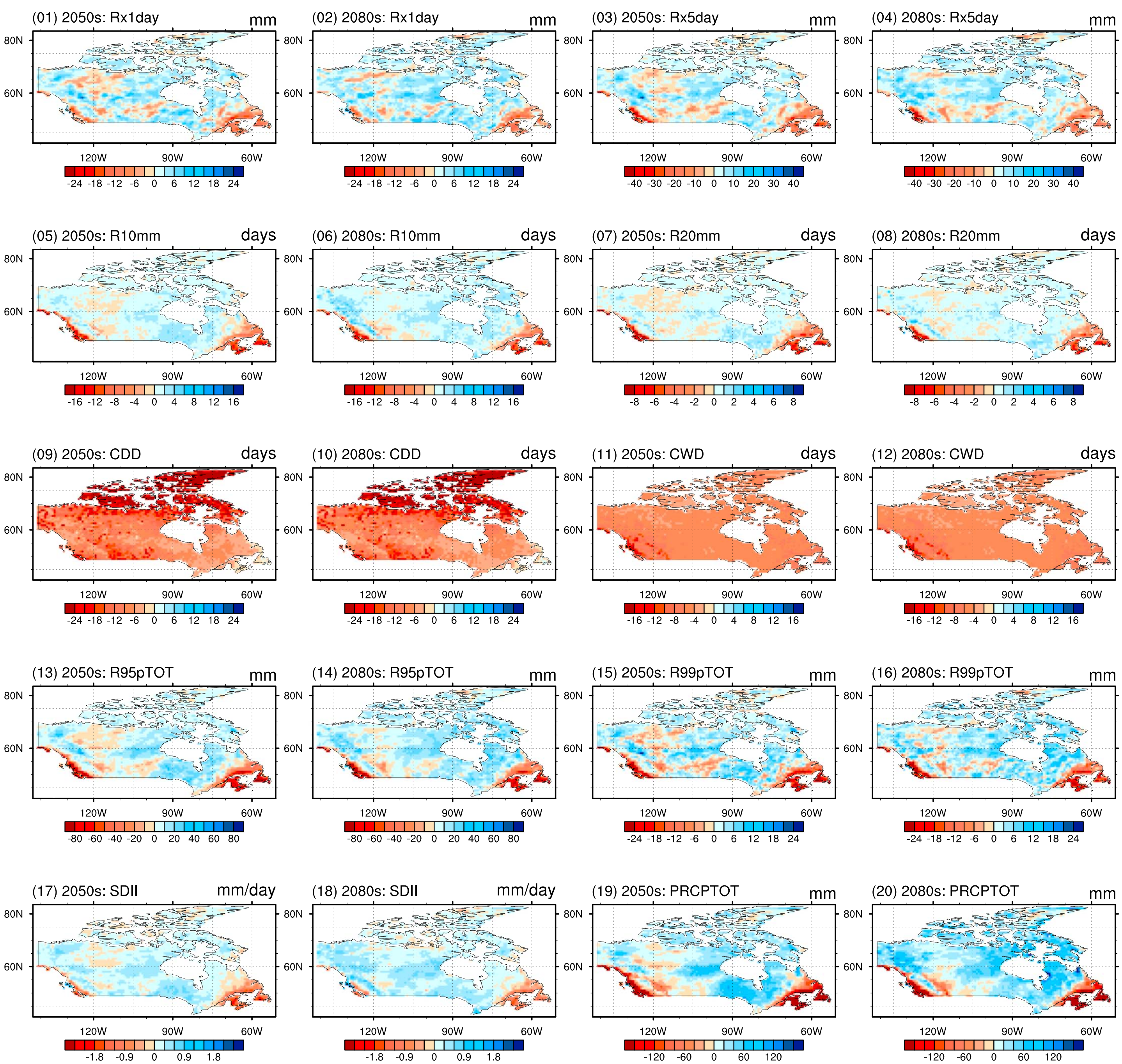

Figure 9. Spatial distribution of the projected changes in extreme indices for the two future periods over Canada under RCP4.5.

projected to slightly increase over the majority regions. In contrast, the PRECIS model simulates a decrease in the averages of CDD and CWD over 10 climatic regions. Moreover, the averages for most extreme indices over PAC and ATL are projected to decrease in the future periods. For example, the averages in Rx5day, R10mm, R20mm, CDD, CWD, R95pTOT, R99pTOT, and PRCPTOT over PAC in the 2050s are expected to decrease by 3.0 mm, 3.1 days, 8.6 days, 9.2 days, 26.2 mm, 7.1 mm, and 132 mm, respectively.

Compared to the RCP4.5 scenario, there are significant increases in the precipitation extreme indices except for the duration indices in the 2050s and 2080s under RCP8.5. The results also indicate that the PRECIS model would amplify the changes in the averages of the indices due to greater GHG concentrations. However, the

10.1029/2017JD027735

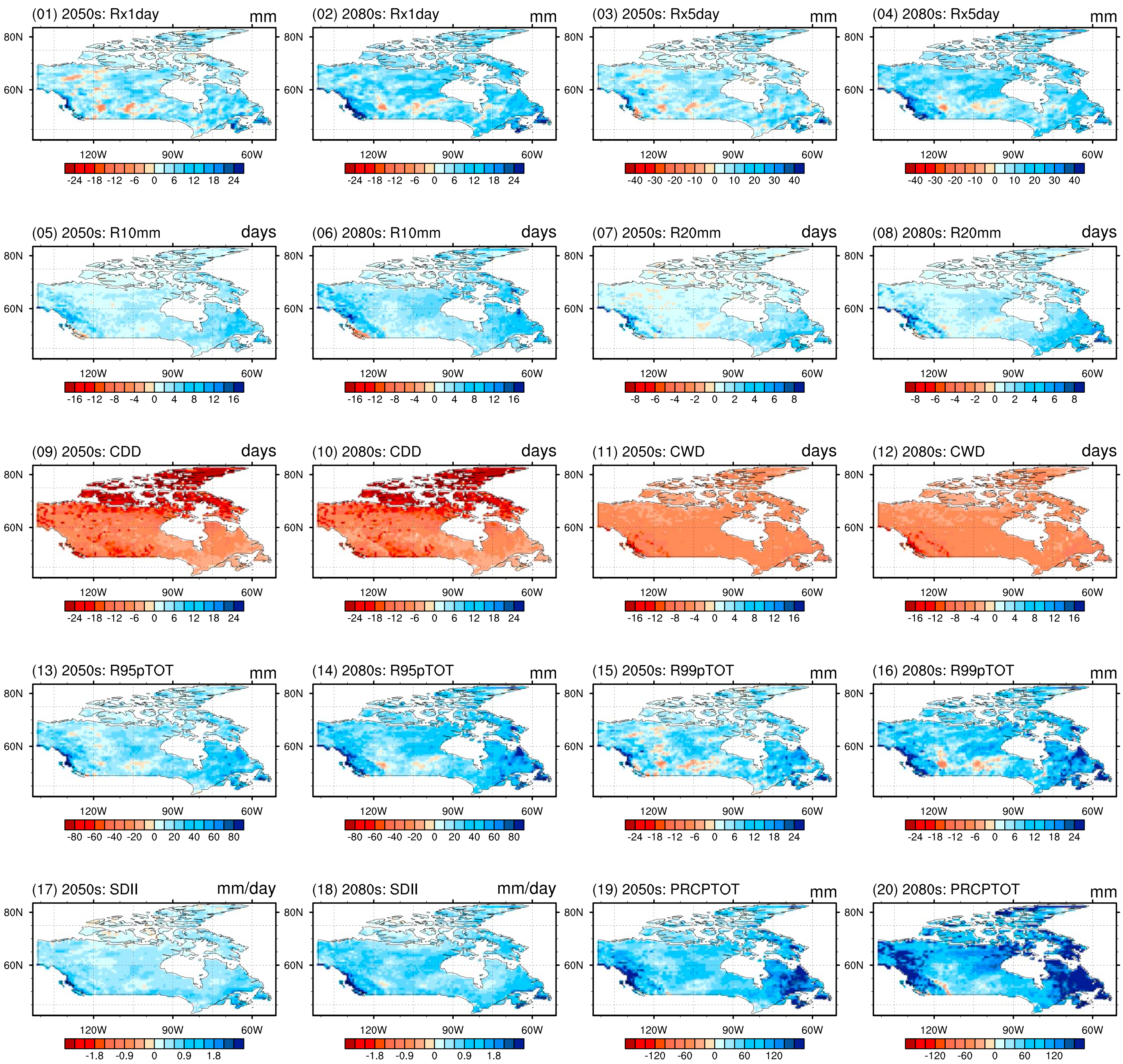

Figure 10. Spatial distribution of the projected changes in extreme indices over Canada for the two future periods under RCP8.5.

PRECIS model projects decreases in the averages of the duration indices over the entirety of climatic regions. For example, as for CDD, the PRECIS simulation projects a significant decrease in averages by as much as 21.5 days in the 2050s and 22 days in the 2080s over ARC. In addition, other two northern regions (i.e., YUK and MAC) are projected to have significant decreases by as much as 13.2 days in the 2050s and 13.5 days in the 2080s under RCP8.5.

3.3. Mechanism of Projected Changes in Precipitation Extremes

In order to further analyze the mechanism governing the projected changes in precipitation extremes for both RCPs, geopotential height, wind, and relative humidity at both 850 and 500 hPa are extracted. In

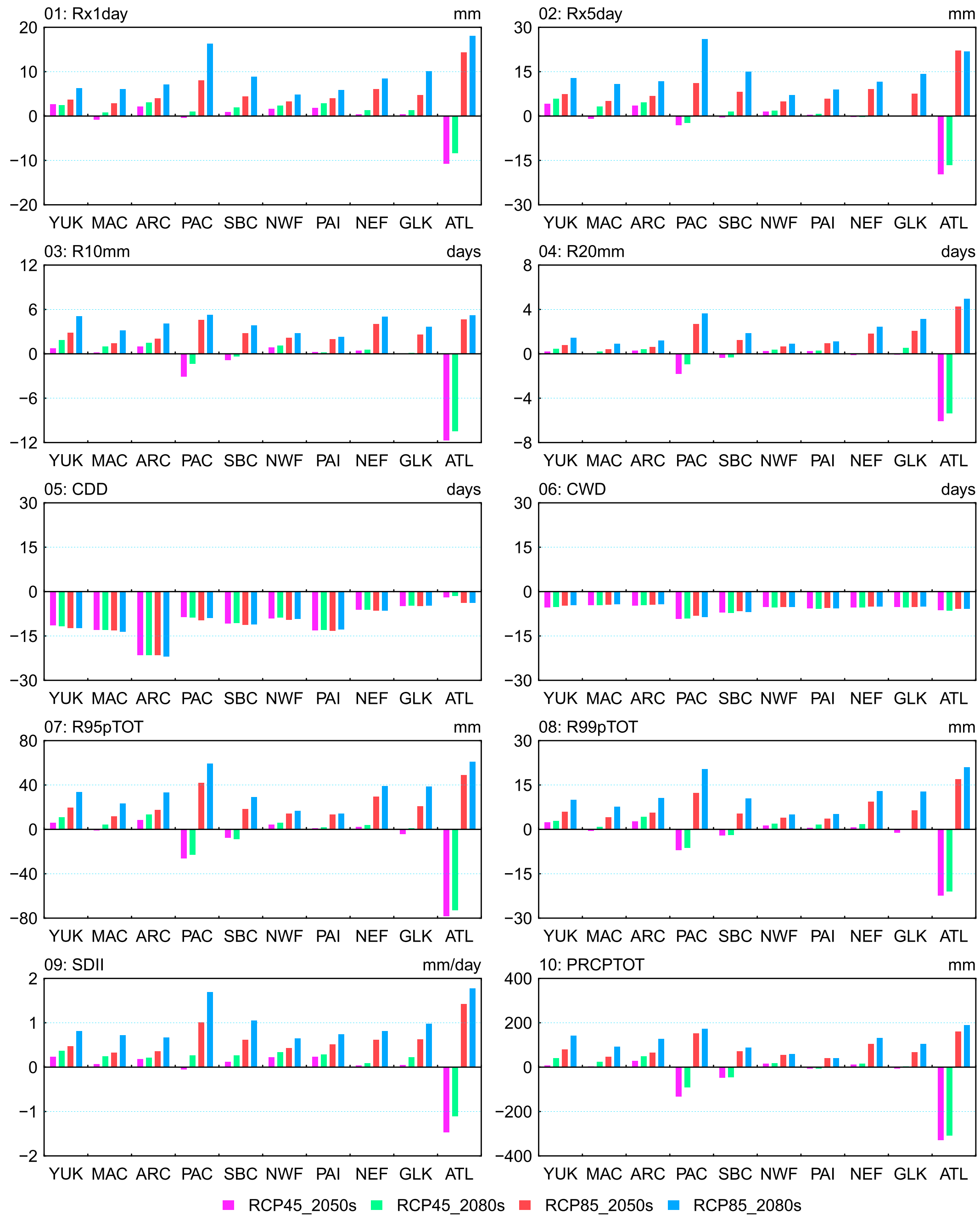

Figure 11. Projected changes in regional averages of extreme indices over 10 climatic regions for both RCPs.

addition, wind velocity, relative humidity, and gravity acceleration, can be employed to calculate water vapor flux. Moreover, intensity of water vapor content transporting trough a unit area could be represented (Zhang et al., 2017). The evaluation results (i.e., Figure 2) reveal that the horizontal transfer of water vapor flux from the North Pacific Ocean, Arctic Ocean, Hudson Bay, Great Lakes, and North Atlantic Ocean contributes to the majority of annual and seasonal total precipitation.

Figure 12 shows the spatial distribution of the projected changes in annual and seasonal mean geopotential height, relative humidity, and wind (*u* and *v*) at 850 hPa over Canada for both RCPs in the two future periods. Compared to the projected changes in annual precipitation, the projected changes in patterns of both annual and seasonal relative humidity are generally similar to those changes in total precipitation in future periods

10.1029/2017JD027735

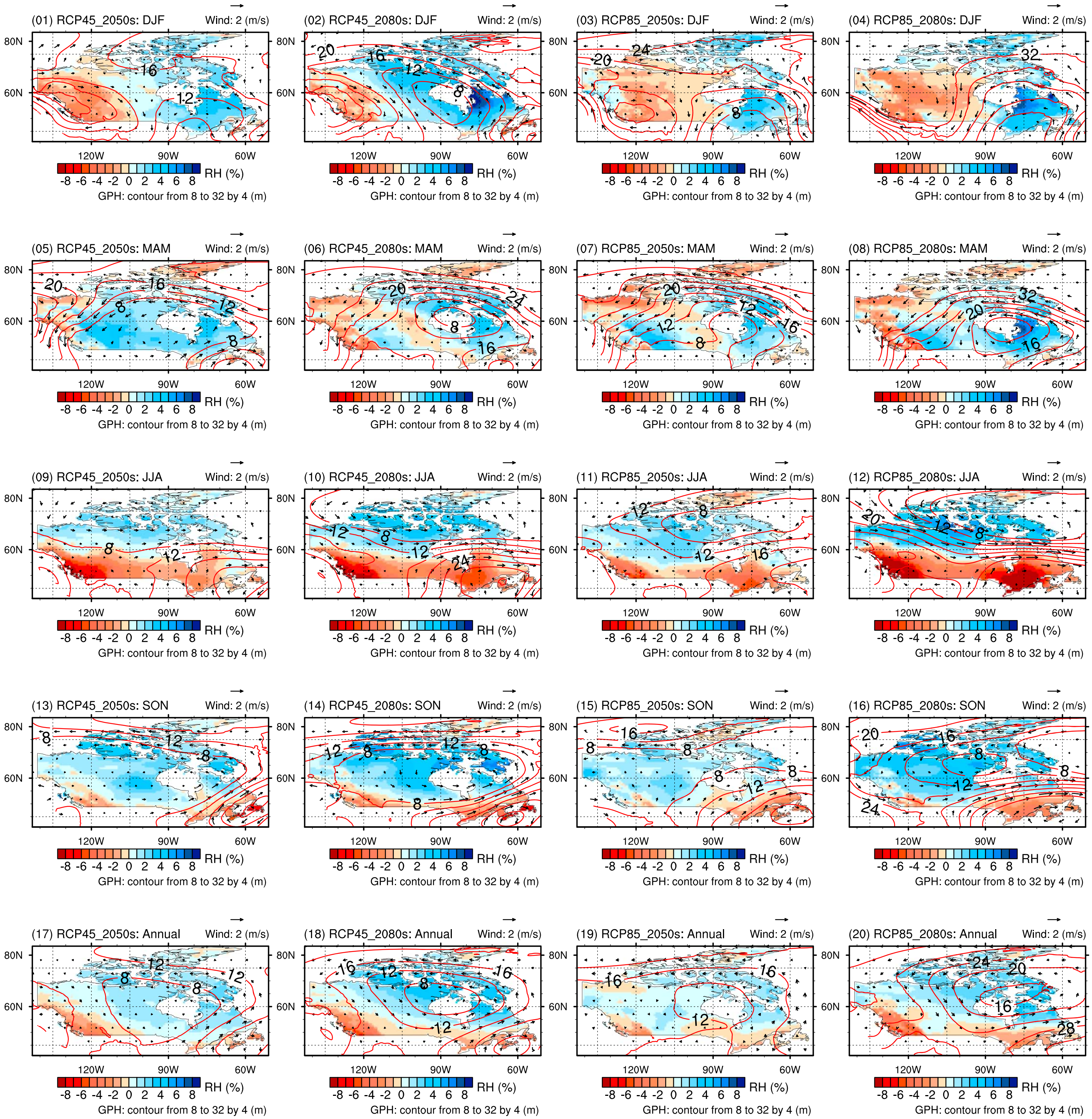

Figure 12. Spatial distribution of the projected changes in annual and seasonal mean geopotential height, relative humidity, and wind (*u* and *v*) at 850 hPa over Canada in the 2050s and 2080s for both RCPs.

for both RCPs. This is consistent with the results of the projected changes in annual and seasonal total precipitation. For example, relative humidity would be projected to decrease less in autumn than in summer over the southern Canada. The results also indicated that the southwest wind would be increased

10.1029/2017JD027735

over the southern Canada in autumn. As a results, more water vapor flux and precipitation would be projected over southern Canada in autumn for the future periods.

It could also be found that the relative humidity is projected to be decreased over the southwestern Canada under RCP4.5. As a consequence, less water vapor in this area would be anticipated in the 2050s and 2080s. However, there are no significant changes in the projected winds under RCP8.5 in the 2050s, while higher GPH would be projected over the southwestern region. This might result in more precipitation regardless of less relative humidity in the future periods. Moreover, the northeast wind is increased over this area in the 2080s under RCP8.5, which might lead to more precipitation due to the cold front. The results also indicated that the precipitation is projected to increase in the rain shadow of the Canadian Rocky Mountains regardless of less relative humidity. Precipitation increases in this area could be contributed from changes in the advection of water to higher elevations and orographic precipitation due to warmer temperature at lower elevation (Williams et al., 1996). According to the precipitation-elevation relationship commonly described as the orographic effect (Daly et al., 1994; Houghton, 1979; Osborn & David, 1977; Schermerhorn, 1967; Smith, 1979), the Canadian Rocky Mountains could increase intensity of cyclonic precipitation by retarding the rate of movement of the storm, leading forced uplift of the air mass (Barry, 1973; Daly et al., 1994). Such increases will have significant impacts on the precipitation extremes. Figure 13 depicts the map of the projected changes in annual mean geopotential height, relative humidity, and wind (*u* and *v*) at 500 hPa over Canada in the 2050s and 2080s for both RCPs. In general, the annual and seasonal relative humidity are projected to decrease in southern Canada and to increase in northern Canada. However, the GPH at 500 hPa would be increased for both RCPs in the future. These factors further evidence the spatial patterns of the projected changes in annual and seasonal total precipitation. Overall, the horizontal water vapor flux associated with the terrain will have a significant effect on the occurrence of precipitation in Canada (Smith et al., 2010). These factors could further affect the projected changes in precipitation extremes in the 2050s and 2080s for both RCPs (Qin & Xie, 2016).

To better understand the influences of these factors on precipitation extremes, vertical wind, and specific humidity are further extracted in the 2050s and 2080s for both RCPs. The Pearson correlation analysis method is then used to explore potential mechanism behind the changes of precipitation extremes. Figure 14 presents the Pearson correlation coefficients between precipitation extreme indices and climate factors including total precipitation (PR), vertical wind (VW), geopotential height (GPH), relative humidity (RH), and specific humidity (SH) from ERA-PRECIS and Had-PRECIS. The results shown in Figures 14-1 and 14-2 indicate that precipitation extreme indices excluding CWD from both ERA-PRECIS and Had-PRECIS show much higher correlations with annual and seasonal total precipitation, mean GPH, and SH, which demonstrate that changes in these factors could have significant impacts on precipitation extremes.

In general, most precipitation extreme indices excluding CWD in the 2050s and 2080s under RCP4.5 are positively correlated with winter total precipitation, autumn relative humidity, and winter specific humidity at a significance level of 0.05. The results also indicate that there are closer relationships among seasonal/annual total precipitation, relative humidity, and specific humidity than other climate factors. Conversely, these indices are negatively correlated with seasonal/annual vertical wind and geopotential height, except for summer GPH with CWD. Strong correlation with both vertical winds and specific humidity at 850 hPa is also consistent with the previous studies (O'Gorman & Schneider, 2009; Qin & Xie, 2016). This is because moisture convergence associated with vertical motion is usually the main process that induces precipitation, which is particularly true for heavy precipitation (Chen et al., 2012; Schneider et al., 2010; Sugiyama et al., 2010). Precipitation increase could be also attributed to the changes in the vertical motion associated with convection due to dynamic contribution (Chen et al., 2012). The correlation analysis results indicated that the changes in magnitudes of annual and seasonal total precipitation would cause changes in the majority of precipitation extreme indices. Moreover, the correlation between these climate factors and precipitation extreme indices is weaker under RCP8.5. This might be due to larger temporal and spatial uncertainties under a higher emission scenario, imposing requirements of more comprehensive understanding and knowledge of the climate system.

Spatial patterns of the projected changes in both extreme and mean precipitation show an agreement with a previous study by Zhou, Huang, Baetz, et al. (2018) who suggested that PRECIS driven by HadGEM2-ES would project larger increases in temperature over the northern area compared to the southwestern region in

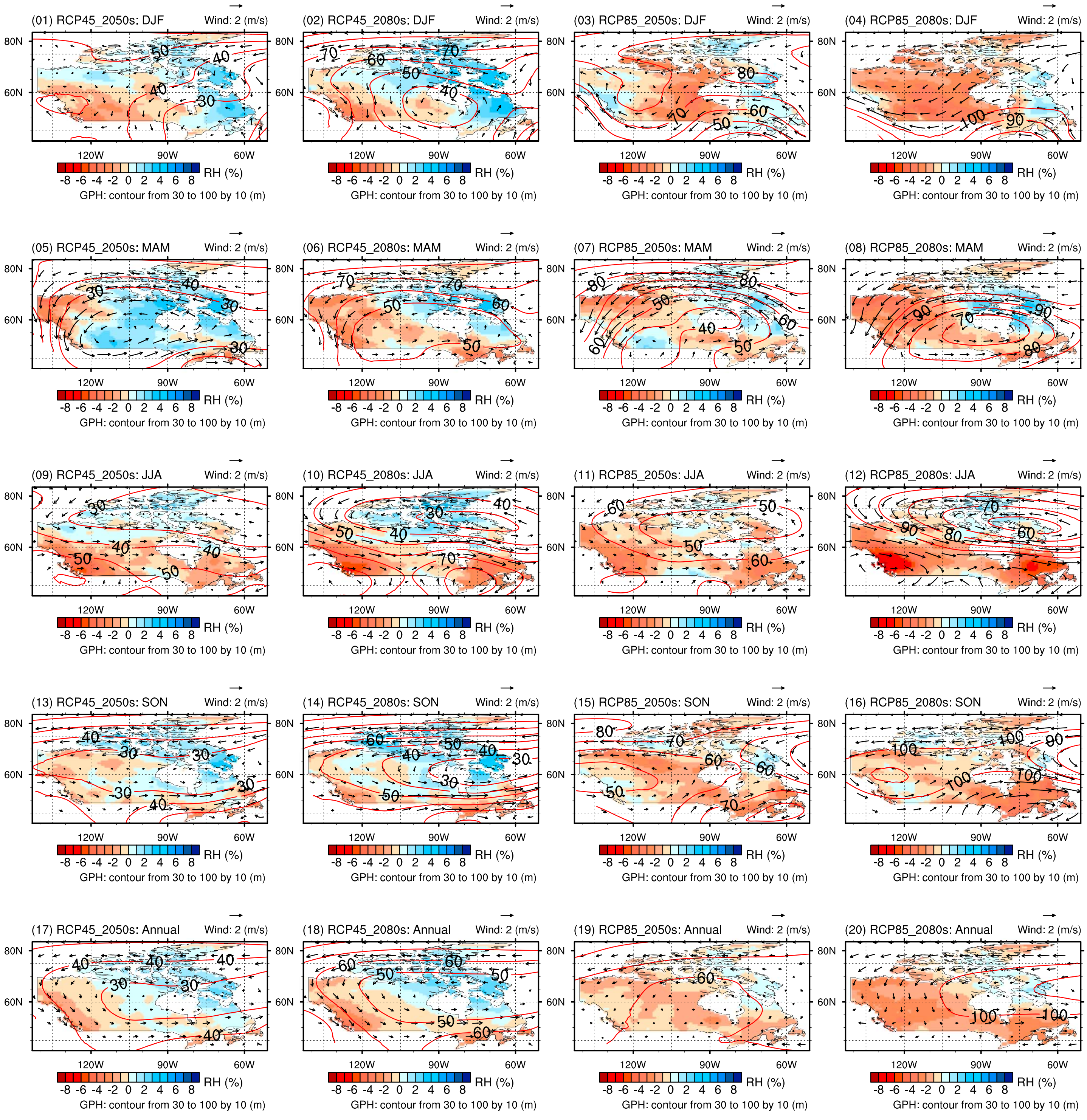

Figure 13. Spatial distribution of the projected changes in annual and seasonal mean geopotential height, relative humidity, and wind (*u* and *v*) at 500 hPa over Canada in the 2050s and 2080s for both RCPs.

Canada. This could be commonly attributed to the changes in saturation vapor pressure due to warmer temperature as described by the Clausius-Clapeyron equation, leading to a significant increase in the atmospheric water content. Such increases would result in a strong positive water vapor feedback. As a consequence, an increase by 7% of vapor content per degree Celsius is expected following the

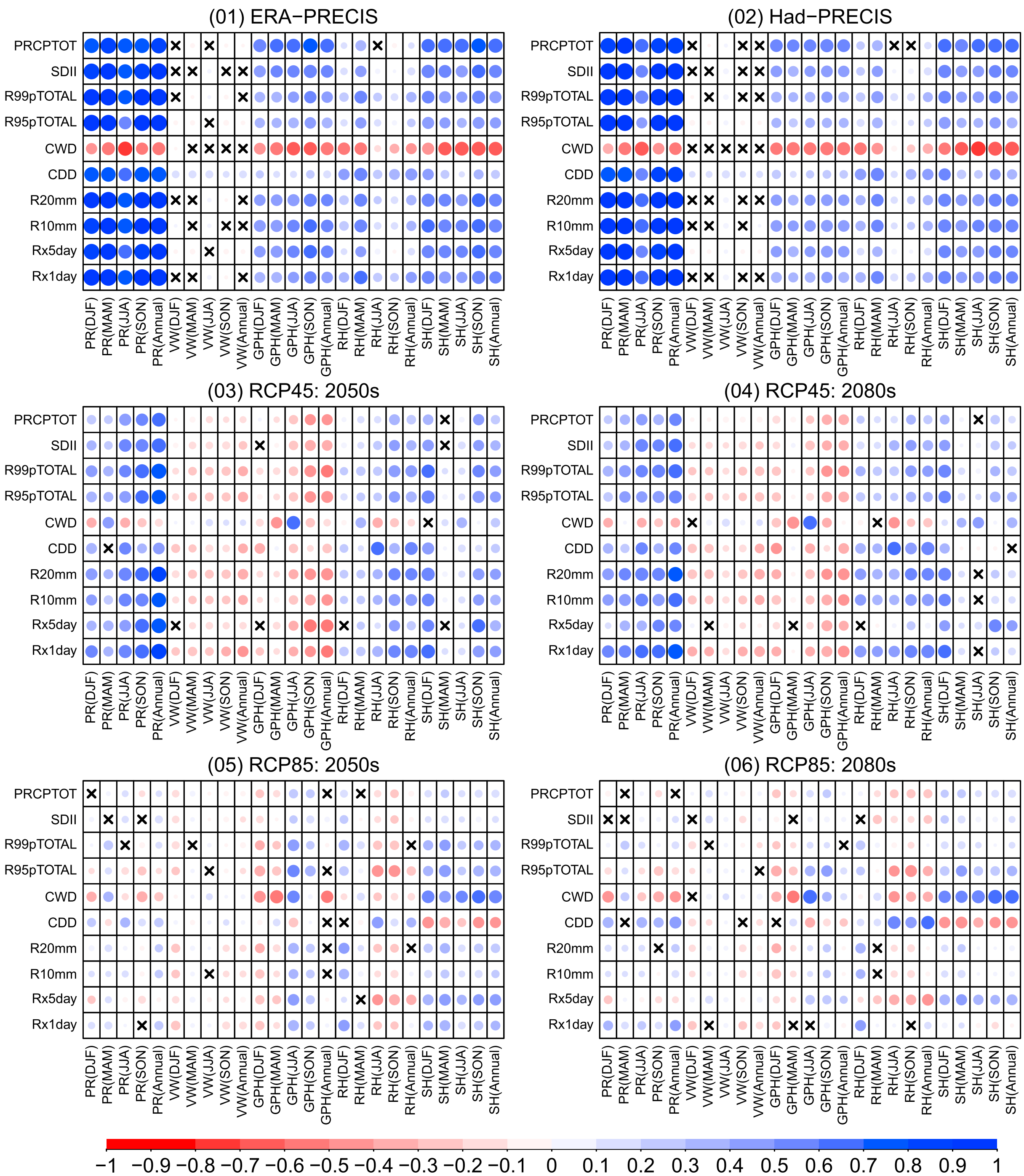

Figure 14. Pearson correlation coefficients between precipitation extreme indices and climate factors (total precipitation, vertical wind, geopotential height, relative humidity, and specific humidity at 850 hPa) from ERA-PRECIS and Had-PRECIS. The correlations with a cross mark are considered to be insignificant since *p* values are large than 0.05.

Clausius-Clapeyron equation (Held & Soden, 2006; Seager et al., 2010). In addition, global warming is likely to intensify the hydrological cycle in multiple ways through increased cloudiness, latent heat fluxes, and intense precipitation events. Changes in circulation could affect precipitation changes through dynamic effects of a strong positive feedback between circulation and convection on moisture convergence (Ma & Xie, 2013; Seager et al., 2010). This will eventually result in increased precipitation and more frequent precipitation extremes in extratropical regions (Betts, 1998; He, 2015; Held & Soden, 2006; Wang, Huang, & Liu, 2014).

10.1029/2017JD027735

The main limitation of this study is that there is only one GCM is used, which is unable to deal with the uncertainties in future projections. However, a majority of uncertainties are associated with the choice of driving GCM, which will have a significant impact on the RCM-simulated precipitation and therefore eventually affect the projected changes in precipitation extremes (Déqué et al., 2007). Such uncertainties can be evaluated and quantified through an ensemble approach. As an efficient method, the ensemble approach is widely employed to explore the full range of multiple projections (Wang, Huang, Lin, et al., 2014), which would advance the understanding of the uncertainties in atmospheric and related processes. Therefore, it is preferable to provide a reliable climate projection with a higher resolution (i.e., 25 km) by dynamically downscaling multiple GCMs (Christensen et al., 2007; Déqué et al., 2007), which would deserve future research efforts.

4. Conclusions

In this study, changes in precipitation extremes over 10 climatic regions in Canada and their mechanism for both RCPs throughout this century were investigated by using the PRECIS model. The performance of PRECIS in hindcasting annual mean and extreme precipitation for the historical period of 1986–2005 was first evaluated through the comparison with observations. Changes in annual mean and extreme precipitation for two future periods (i.e., 2036–2065 and 2066–2095) were then analyzed to explore how regional climate over 10 climatic regions would respond to global warming. Moreover, The driving factors and inherent mechanism governing the projected changes in precipitation extremes were revealed through a comprehensive analysis of the potential climate factors, as well as their correlations and interactions with precipitation extremes.

The results indicated that ERA-PRECIS and Had-PRECIS could reasonably reproduce the patterns and magnitudes of precipitation extremes over Canada through comparison with the observations. However, we found that PRECIS could not fully capture formation and precipitation of convective clouds and large-scale clouds over the southeastern region as seen from its slightly poor performance in simulating precipitation extremes. The projected changes in precipitation extremes suggest that there are obvious increasing trends over the majority of climatic regions for the magnitude of precipitation extreme indices except for the duration indices. In addition to the increasing trends, the changes in magnitudes of the precipitation extreme indices show a similar spatial pattern associated with the changes in annual total precipitation. Moreover, the averages of the projected precipitation extremes over the climatic regions in Canada would be generally increased for the 2050s and 2080s under RCP4.5, and these increases would be amplified under RCP8.5 due to larger GHG concentrations.

The mechanism governing the projected changes in the precipitation extremes for both RCPs in the future periods was analyzed through a comprehensive investigation of the potential climate factors such as geopotential height, wind, and relative humidity at both 850 and 500 hPa. The projected changes in total precipitation are mainly consequences of future changes in wind velocity and relative humidity and therefore changes in horizontal water vapor flux. It is suggested that these factors would have a significant effect on the occurrence of precipitation in Canada. The Pearson correlation analysis method was then used to explore mechanism behind the changes of precipitation extremes. Most precipitation extreme indices excluding CWD in the 2050s and 2080s under RCP4.5 are positively correlated with total precipitation, relative humidity, and specific humidity at a significance level of 0.05. The results also indicate that there are closer relationships among seasonal/annual total precipitation, relative humidity, and specific humidity than other climate factors. Conversely, these indices are negatively correlated with seasonal/annual vertical wind and geopotential height, except for summer GPH with CWD. Moreover, the correlation between the climate factors and precipitation extremes is weaker under RCP8.5 due to larger temporal and spatial uncertainties under a higher emission scenario. The correlation analysis results indicate that the changes in the majority of precipitation extremes are commonly attributed to the changes in the saturation vapor pressure due to warmer temperature as described by the Clausius-Clapeyron equation. Meanwhile, changes in circulation could affect precipitation changes through dynamic effects of a strong positive feedback. The projected changes and revealed mechanism in precipitation extremes over Canada can help understand atmospheric properties and processes at regional and local scales.

Acknowledgments

We are very grateful to the Editor, L. Ruby Leung, and two anonymous reviewers for their insightful suggestions in improving the quality of this paper. This research was supported by the National Key Research and Development Plan (2016YFA0601502 and 2016YFC0502800), the Natural Sciences Foundation (51520105013 and 51679087), the 111 Program (B14008), and the Natural Science and Engineering Research Council of Canada. The datasets used in this study are available from the Canada Climate Change Data Portal (http://canadaccdp.ca/).

References

Bao, J., Feng, J., & Wang, Y. (2015). Dynamical downscaling simulation and future projection of precipitation over China. *Journal of Geophysical Research: Atmospheres*, *120*, 8227–8243. https://doi.org/10.1002/2015JD023275

Barry, R. G. (1973). A climatological transect on the east slope of the Front Range, Colorado. *Arctic and Alpine Research*, *5*(2), 89–110. https://doi.org/10.2307/1550251

Betts, A. K. (1998). Climate-convection feedbacks: Some further issues. *Climatic Change*, *39*(1), 35–38. https://doi.org/10.1023/A:1005323805826

Centella-Artola, A., Taylor, M. A., Bezanilla-Morlot, A., Martinez-Castro, D., Campbell, J. D., Stephenson, T. S., & Vichot, A. (2015). Assessing the effect of domain size over the Caribbean region using the PRECIS regional climate model. *Climate Dynamics*, *44*(7-8), 1901–1918. https://doi.org/10.1007/s00382-014-2272-8

Environment and Climate Change Canada (2016). Impacts of climate change. Retrieved from https://ec.gc.ca/sc-cs/default.asp?lang=En&n=A5F83C26-1, Accessed 15 August 2016

Intergovernmental Panel on Climate Change (2013). In T. F. Stocker, et al. (Eds.), *Climate change 2013: The physical science basis. Contribution of Working Group I to the Fifth Assessment Report of the Intergovernmental Panel on Climate Change* (p. 1535). Cambridge, UK: Cambridge University Press.

Chen, C.-A., Chou, C., & Chen, C.-T. (2012). Regional perspective on mechanisms for tropical precipitation frequency and intensity under global warming. *Journal of Climate*, *25*(24), 8487–8501. https://doi.org/10.1175/JCLI-D-12-00096.1

Christensen, J. H., Carter, T. R., Rummukainen, M., & Amanatidis, G. (2007). Evaluating the performance and utility of regional climate models: The PRUDENCE project. *Climatic Change*, *81*(S1), 1–6. https://doi.org/10.1007/s10584-006-9211-6

Cox, P., Betts, R., Bunton, C., Essery, R., Rowntree, P., & Smith, J. (1999). The impact of new land surface physics on the GCM simulation of climate and climate sensitivity. *Climate Dynamics*, *15*(3), 183–203. https://doi.org/10.1007/s003820050276

Daly, C., Neilson, R. P., & Phillips, D. L. (1994). A statistical-topographic model for mapping climatological precipitation over mountainous terrain. *Journal of Applied Meteorology*, *33*(2), 140–158. https://doi.org/10.1175/1520-0450(1994)033%3C0140:ASTMFM%3E2.0.CO;2

Denis B., Laprise R., Caya D., & Côté J. (2002). Downscaling ability of one-way nested regional climate models: The Big-Brother experiment. *Climate Dynamics*, *18*, 627–646.

Déqué, M., Rowell, D., Lüthi, D., Giorgi, F., Christensen, J., Rockel, B., et al. (2007). An intercomparison of regional climate simulations for Europe: Assessing uncertainties in model projections. *Climatic Change*, *81*(S1), 53–70. https://doi.org/10.1007/s10584-006-9228-x

Fan, Y. R., Huang, G., Baetz, B. W., Li, Y. P., & Huang, K. (2017). Development of Copula-based Particle Filter (CopPF) approach for hydrologic data assimilation under consideration of parameter interdependence. *Water Resources Research*, *53*, 4850–4875. https://doi.org/10.1002/2016WR020144

Frich, P., Alexander, L. V., Della-Marta, P., Gleason, B., Haylock, M., Tank, A. K., & Peterson, T. (2002). Observed coherent changes in climatic extremes during the second half of the twentieth century. *Climate Research*, *19*, 193–212. https://doi.org/10.3354/cr019193

Hartmann, D. L., Tank, A. M. K., Rusticucci, M., Alexander, L. V., Brönnimann, S., Charabi, Y. A. R., et al. (2013). Observations: Atmosphere and surface. In T. F. Stocker, et al. (Eds.), *Climate change 2013:The physical science basis: Working Group I Contribution to the Fifth Assessment Report of the Intergovernmental Panel on Climate Change* (pp. 159–254). Cambridge, UK: Cambridge University Press.

He, J. (2015). *Mechanisms of changes in precipitation and atmospheric circulation from anthropogenic forcing*. Coral Gables, FL: University of Miami.

Held, I. M., & Soden, B. J. (2006). Robust responses of the hydrological cycle to global warming. *Journal of Climate*, *19*(21), 5686–5699. https://doi.org/10.1175/JCLI3990.1

Houghton, J. G. (1979). A model for orographic precipitation in the north-central Great Basin. *Monthly Weather Review*, *107*(11), 1462–1475. https://doi.org/10.1175/1520-0493(1979)107%3C1462:AMFOPI%3E2.0.CO;2

Janjić, Z. I. (1994). The step-mountain eta coordinate model: Further developments of the convection, viscous sublayer, and turbulence closure schemes. *Monthly Weather Review*, *122*(5), 927–945. https://doi.org/10.1175/1520-0493(1994)122%3C0927:TSMECM%3E2.0.CO;2

Jeong, D. I., Sushama, L., Diro, G. T., & Khaliq, M. N. (2016). Projected changes to winter temperature characteristics over Canada based on an RCM ensemble. *Climate Dynamics*, *47*(5-6), 1351–1366. https://doi.org/10.1007/s00382-015-2906-5

Jeong, D. I., Sushama, L., Diro, G. T., Khaliq, M. N., Beltrami, H., & Caya, D. (2016). Projected changes to high temperature events for Canada based on a regional climate model ensemble. *Climate Dynamics*, *46*(9-10), 3163–3180. https://doi.org/10.1007/s00382-015-2759-y

Jones, R., & Hassell, D. (2004). *Generating high resolution climate change scenarios using PRECIS*. Exeter, UK: Met Office Hadley Centre.

Jones, R., Murphy, J., & Noguer, M. (1995). Simulation of climate change over Europe using a nested regional-climate model. I: Assessment of control climate, including sensitivity to location of lateral boundaries. *Quarterly Journal of the Royal Meteorological Society*, *121*, 1413–1449.

Kennedy, A. D., Dong, X., Xi, B., Xie, S., Zhang, Y., & Chen, J. (2011). A comparison of MERRA and NARR reanalyses with the DOE ARM SGP data. *Journal of Climate*, *24*(17), 4541–4557. https://doi.org/10.1175/2011JCLI3978.1

Li, J., Zhang, Q., Chen, Y. D., & Singh, V. P. (2013). GCMs-based spatiotemporal evolution of climate extremes during the 21st century in China. *Journal of Geophysical Research: Atmospheres*, *118*, 11,017–11,035. https://doi.org/10.1002/jgrd.50851

Ma, J., & Xie, S.-P. (2013). Regional patterns of sea surface temperature change: A source of uncertainty in future projections of precipitation and atmospheric circulation. *Journal of Climate*, *26*(8), 2482–2501. https://doi.org/10.1175/JCLI-D-12-00283.1

Mailhot, A., Beauregard, I., Talbot, G., Caya, D., & Biner, S. (2012). Future changes in intense precipitation over Canada assessed from multi-model NARCCAP ensemble simulations. *International Journal of Climatology*, *32*(8), 1151–1163. https://doi.org/10.1002/joc.2343

Maurer, E. P., Brekke, L., Pruitt, T., & Duffy, P. B. (2007). Fine-resolution climate projections enhance regional climate change impact studies. *Eos, Transactions American Geophysical Union*, *88*(47), 504–504. https://doi.org/10.1029/2007EO470006

Mesinger, F., Janjić, Z. I., Ničković, S., Gavrilov, D., & Deaven, D. G. (1988). The step-mountain coordinate: Model description and performance for cases of Alpine lee cyclogenesis and for a case of an Appalachian redevelopment. *Monthly Weather Review*, *116*(7), 1493–1518. https://doi.org/10.1175/1520-0493(1988)116%3C1493:TSMCMD%3E2.0.CO;2

Mladjic, B., Sushama, L., Khaliq, M., Laprise, R., Caya, D., & Roy, R. (2011). Canadian RCM projected changes to extreme precipitation characteristics over Canada. *Journal of Climate*, *24*(10), 2565–2584. https://doi.org/10.1175/2010JCLI3937.1

O'Gorman, P. A., & Schneider, T. (2009). The physical basis for increases in precipitation extremes in simulations of 21st-century climate change. *Proceedings of the National Academy of Sciences of the United States of America*, *106*(35), 14,773–14,777. https://doi.org/10.1073/pnas.0907610106

Osborn, H. B., & David, D. R. (1977). Distribution of precipitation on rugged terrain in central Arizona. In *Hydrology and water resources in Arizona and the Southwest* (pp. 73–79). Las Vegas, NV: Arizona-Nevada Academy of Science.

Plummer, D., Caya, D., Frigon, A., Côté, H., Giguère, M., Paquin, D., et al. (2006). Climate and climate change over North America as simulated by the Canadian RCM. *Journal of Climate*, *19*(13), 3112–3132. https://doi.org/10.1175/JCLI3769.1

Qin, P., & Xie, Z. (2016). Detecting changes in future precipitation extremes over eight river basins in China using RegCM4 downscaling. *Journal of Geophysical Research: Atmospheres*, *121*, 6802–6821. https://doi.org/10.1002/2016JD024776

Saha, S., Moorthi, S., Wu, X., Wang, J., Nadiga, S., Tripp, P., et al. (2014). The NCEP climate forecast system version 2. *Journal of Climate*, *27*(6), 2185–2208. https://doi.org/10.1175/JCLI-D-12-00823.1

Schermerhorn, V. P. (1967). Relations between topography and annual precipitation in western Oregon and Washington. *Water Resources Research*, *3*(3), 707–711. https://doi.org/10.1029/WR003i003p00707

Schneider, T., O'Gorman, P. A., & Levine, X. J. (2010). Water vapor and the dynamics of climate changes. *Reviews of Geophysics*, *48*, RG3001. https://doi.org/10.1029/2009RG000302

Seager, R., Naik, N., & Vecchi, G. A. (2010). Thermodynamic and dynamic mechanisms for large-scale changes in the hydrological cycle in response to global warming. *Journal of Climate*, *23*(17), 4651–4668. https://doi.org/10.1175/2010JCLI3655.1

Seager, R., Ting, M., Held, I., Kushnir, Y., Lu, J., Vecchi, G., et al. (2007). Model projections of an imminent transition to a more arid climate in southwestern North America. *Science*, *316*(5828), 1181–1184. https://doi.org/10.1126/science.1139601

Shabbar, A., & Bonsal, B. (2003). An assessment of changes in winter cold and warm spells over Canada. *Natural Hazards*, *29*(2), 173–188. https://doi.org/10.1023/A:1023639209987

Sillmann, J., Kharin, V., Zhang, X., Zwiers, F., & Bronaugh, D. (2013). Climate extremes indices in the CMIP5 multimodel ensemble: Part 1. Model evaluation in the present climate. *Journal of Geophysical Research: Atmospheres*, *118*, 1716–1733. https://doi.org/10.1002/jgrd.50203

Sillmann, J., Kharin, V., Zwiers, F., Zhang, X., & Bronaugh, D. (2013). Climate extremes indices in the CMIP5 multimodel ensemble: Part 2. Future climate projections. *Journal of Geophysical Research: Atmospheres*, *118*, 2473–2493. https://doi.org/10.1002/jgrd.50188

Smith, B. L., Yuter, S. E., Neiman, P. J., & Kingsmill, D. (2010). Water vapor fluxes and orographic precipitation over northern California associated with a landfalling atmospheric river. *Monthly Weather Review*, *138*(1), 74–100. https://doi.org/10.1175/2009MWR2939.1

Smith, R. B. (1979). The influence of mountains on the atmosphere. *Advances in Geophysics*, *21*, 87–230. https://doi.org/10.1016/S0065-2687(08)60262-9

Sugiyama, M., Shiogama, H., & Emori, S. (2010). Precipitation extreme changes exceeding moisture content increases in MIROC and IPCC climate models. *Proceedings of the National Academy of Sciences of the United States of America*, *107*(2), 571–575. https://doi.org/10.1073/pnas.0903186107

Sushama, L., Khaliq, N., & Laprise, R. (2010). Dry spell characteristics over Canada in a changing climate as simulated by the Canadian RCM. *Global and Planetary Change*, *74*(1), 1–14. https://doi.org/10.1016/j.gloplacha.2010.07.004

Taylor, K. E. (2001). Summarizing multiple aspects of model performance in a single diagram. *Journal of Geophysical Research*, *106*(D7), 7183–7192. https://doi.org/10.1029/2000JD900719

Van Vuuren, D. P., Edmonds, J., Kainuma, M., Riahi, K., Thomson, A., Hibbard, K., et al. (2011). The representative concentration pathways: An overview. *Climatic Change*, *109*(1-2), 5–31. https://doi.org/10.1007/s10584-011-0148-z

Wang, X., Huang, G., Lin, Q., & Liu, J. (2014). High-resolution probabilistic projections of temperature changes over Ontario, Canada. *Journal of Climate*, *27*(14), 5259–5284. https://doi.org/10.1175/JCLI-D-13-00717.1

Wang, X., Huang, G., & Liu, J. (2014). Projected increases in intensity and frequency of rainfall extremes through a regional climate modeling approach. *Journal of Geophysical Research: Atmospheres*, *119*, 13,271–13,286. https://doi.org/10.1002/2014JD022564

Wang, X., Huang, G., Liu, J., Li, Z., & Zhao, S. (2015). Ensemble projections of regional climatic changes over Ontario, Canada. *Journal of Climate*, *28*(18), 7327–7346. https://doi.org/10.1175/JCLI-D-15-0185.1

Williams, M. W., Losleben, M., Caine, N., & Greenland, D. (1996). Changes in climate and hydrochemical responses in a high-elevation catchment in the Rocky Mountains, USA. *Limnology and Oceanography*, *41*(5), 939–946. https://doi.org/10.4319/lo.1996.41.5.0939

Wilson S., Hassell D., Hein D., Jones R., & Taylor R. (2005). Installing and using the Hadley Centre regional climate modelling system, PRECIS. Version 1:157.

Zhang, Q., Zheng, Y., Singh, V. P., Luo, M., & Xie, Z. (2017). Summer extreme precipitation in eastern China: Mechanisms and impacts. *Journal of Geophysical Research: Atmospheres*, *122*, 2766–2778. https://doi.org/10.1002/2016JD025913

Zhou, X., Huang, G., Baetz, B. W., Wang, X., & Cheng, G. (2018). PRECIS-projected increases in temperature and precipitation over Canada. *Quarterly Journal of the Royal Meteorological Society*, *144*(711), 588–603. https://doi.org/10.1002/qj.3231

Zhou, X., Huang, G., Wang, X., & Cheng, G. (2018). Dynamically-downscaled temperature and precipitation changes over Saskatchewan using the PRECIS model. *Climate Dynamics*, *50*(3-4), 1321–1334. https://doi.org/10.1007/s00382-017-3687-9

Zhou, X., Huang, G., Wang, X., Fan, Y., & Cheng, G. (2017). A coupled dynamical-copula downscaling approach for temperature projections over the Canadian Prairies. *Climate Dynamics*, 1–19.